

The labile fraction of suspended matter in the Loire River (France): multi-element chemistry and isotopic (Rb–Sr and C–O) systematics

Philippe Négrel^{a,*}, Cécile Grosbois^{a,b}, Wolfram Kloppmann^a

^a BRGM Research Division, Avenue C. Guillemin, BP 6009, 45060 Orléans Cedex 02, France

^b Université de Tours, G.E.E.A.C. Faculté des Sciences et Techniques, Parc de Grandmont, 37200 Tours, France

Received 8 April 1999; accepted 12 November 1999

Abstract

Suspended particulate matter transported by the Loire River (France) comprises mainly quartz and K-feldspar during periods of high river flow, with an increase in calcite contents during periods of low flow. We studied the labile fraction (leached by HCl 0.2 N) associated with the suspended matter transported by the upper Loire River. The acid extractable matter (AEM) concentrations in the Loire exhibit a wide range from 8% during high-flow conditions in the river to 47% during the low-flow conditions. The dispersion of AEM data differentiates two fields; one related to a domain where CaCO₃ precipitation is possible, and the other related to a domain where erosion is dominant. The concentrations of trace elements and REE fluctuate widely and generally decrease with increasing AEM concentrations. A middle REE (MREE) enrichment over the LREE and HREE is observed which can be related to Fe–Mn oxide coatings developed on the clastic particles.

The ⁸⁷Sr/⁸⁶Sr ratio varies from 0.710582 to 0.711472 and displays two different trends when plotted against AEM abundance, again reflecting varying contributions from two main end-members. The hydrous Fe–Mn oxides have the lowest ⁸⁷Sr/⁸⁶Sr ratio (≈ 0.7105) and the carbonates have the highest ⁸⁷Sr/⁸⁶Sr ratio (≈ 0.7115). The highest ⁸⁷Sr/⁸⁶Sr ratios of AEM, obtained during the period of authigenic calcite precipitation, agree with values measured for the dissolved Sr over the same period. During the period where erosion dominates, the ⁸⁷Sr/⁸⁶Sr ratio of the hydrous Fe–Mn oxide end-member diverges from the mean value of the dissolved load of the Loire River. This implies that the oxides were formed in water with a lower ⁸⁷Sr/⁸⁶Sr ratio, suggesting that (i) the location of oxide precipitation is upland, and (ii) the oxides conserve their Sr isotope signature during transport by the river and do not re-equilibrate with local waters during transport.

Stable carbon and oxygen isotope compositions of the carbonate fraction of the AEM during low-flow conditions are consistent with authigenic calcite formation in isotopic equilibrium with Loire River water. At high-flow conditions we observe an isotopic enrichment that may reflect a higher proportion of atmospheric CO₂ within the river waters at this time, or a contribution of detrital carbonate material from marine sediments exposed in the watershed, or secondary calcite derived from eroded soils. © 2000 Elsevier Science B.V. All rights reserved.

Keywords: Suspended matter; Sr isotopic ratio; Rare earth elements, mixing model; Authigenic calcite, erosion

* Corresponding author.

E-mail address: p.negrel@brgm.fr (P. Négrel).

1. Introduction

The residual products of chemical and mechanical weathering that are carried by rivers towards the ocean may be divided into the suspended load, (typically smaller than a few microns in diameter), and the bed load, which represents the coarse fraction in bed sediments (Meade et al., 1990). This solid matter is an important vector for the movement of trace metals within the hydrological cycle through a range of adsorption and precipitation mechanisms.

The natural chemical composition of bed sediments in small catchments has been reported for various lithologies (Albarède and Semhi, 1995, Négrel and Deschamps, 1996) and contamination (by trace metals) has been intensively studied in small catchments draining industrial areas (Prohic and Juracic, 1989). Chester et al. (1985) summarized the classification of elements in sediments into environmentally meaningful categories that distinguish between non-residual (adsorbed onto sediment load or onto organic matter) and residual (virtually insoluble) trace elements.

This work focuses on the labile fraction associated with the suspended particulate matter carried by the Loire River and previously investigated by Négrel and Grosbois (1999). Determination of the geochemical behavior of a variety of elements facilitates the study of the role of the labile fraction and its capacity to transport pollutant elements. One objective of this study was to determine the temporal variations of chemical species bound to the suspended matter during a complete hydrological cycle. In addition, we have attempted to trace the origin of the chemical species in the labile fraction through radiogenic- and stable-isotope analyses.

2. Location and description of the Loire catchment

The Loire River in central France is 1010 km long and drains an area of 117,800 km² characterized by a varied topography (Fig. 1). The bedrock composition of the upstream section of the catchment comprises older plutonic rocks (granite, gneiss and mica schist, 500 to 300 Ma) and a large volcanic area that represents 46% of the total basin surface (BRGM,

1996). In the intermediate part of the catchment, the sedimentary series of the Paris Basin consists primarily of carbonate deposits (200 to 6 Ma).

The Loire is one of the principal European riverine inputs of water to the Atlantic Ocean (26 10⁹ m³ yr⁻¹, Figueres et al., 1985). The solid load ranges from 10⁶ (Figueres et al., 1985) to 4.3 10⁶ t yr⁻¹ (Négrel, 1997), with the suspended load representing 3% of the total suspended sediment load for rivers draining western Europe (Milliman and Meade, 1983). Near the city of Orléans, large variations in water discharge are observed between the summer low stage (around 50 m³ s⁻¹) and the winter high stage (> 1000 m³ s⁻¹).

3. Suspended matter sampling and analysis

3.1. Sampling

The drainage basin, upstream of the sampling site at Orléans represents 34% of the total Loire catchment, that includes in the entire silicate basement of the Massif Central and about 24% of the total sedimentary area. The sampling of the Loire River was divided into two periods (Négrel and Grosbois, 1999) and this study focuses on the second period, from May 1995 to March 1996 where the river was sampled between once a week and three times a week, according to the river discharge. Each sample, i.e., 60 to 90 l of water, was collected in pre-cleaned polypropylene containers from the centre of the main channel of the river (Négrel and Grosbois, 1999). Total suspended matter concentrations (in mg l⁻¹) were determined by weighing dried acetate cellulose membranes (0.22 µm) before and after the filtration of 1 l of water. The suspended matter samples were obtained by settling the sample over several days, oven-drying at 70°C, powdering and dry-sieving through a 165-µm nylon mesh to extract fresh coarse organic matter (wood, etc). Samples are referred to in the results as jlo - x, where x represents the number of each individual sample.

3.2. Extraction of the trace elements

The mechanism by which metals and other chemical species are bound onto solid matter (soils and

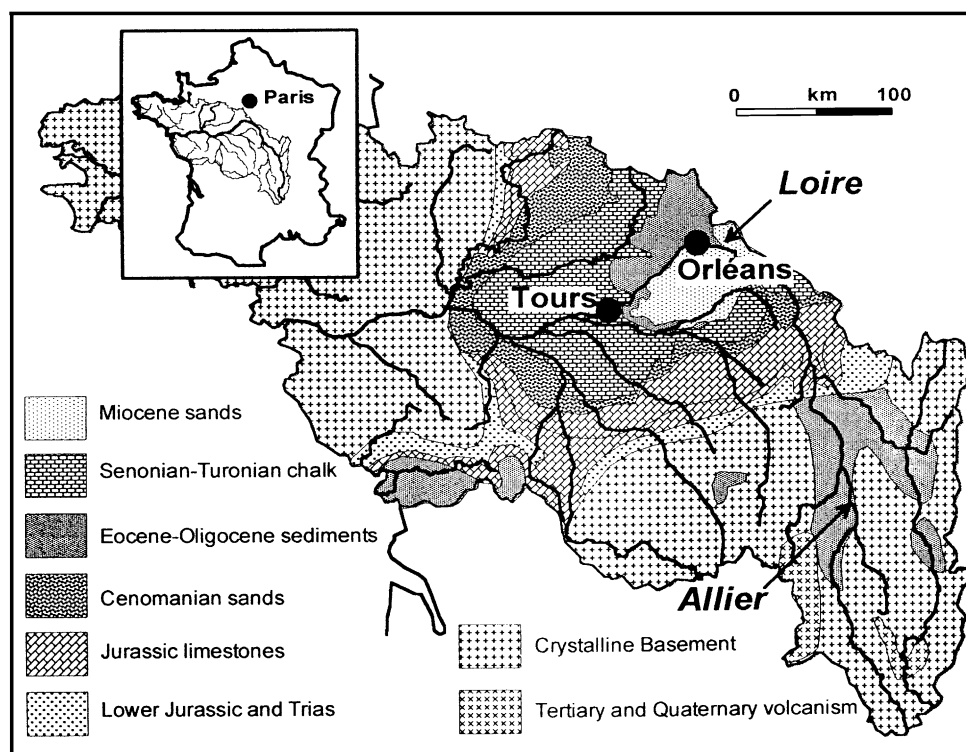


Fig. 1. Simplified geological map of the upper Loire River catchment.

sediments) may exert an important control on their geochemical behaviour. Although numerous extraction schemes have been used to discriminate between geochemical phases, they follow two main approaches (Breward et al., 1996) that differ mainly in their complexity. The simpler method involves separating a labile fraction from a residual fraction (Chester et al., 1985; Elderfield and Sholkovitz, 1987), whereas the more complex approach involves using various reagents for the sequential removal of adsorbed elements, followed by carbonates, phosphates and Fe/Mn oxides (Tessier et al., 1979; Leleyter and Probst, 1998). However, studies since the 1980s have revealed limitations associated with the use of leaching techniques (e.g., Sholkovitz, 1989). One of the main criticisms concerns the re-adsorption of the extracted elements back onto sediments, even at low pH (< 2.0). Sholkovitz (1989) studied artifacts induced during the leaching of sedi-

ments for rare earth element (REE) determination and concluded that 100% recovery of labile REE could be obtained by leaching with HCl (> 0.2 N). In the present study the labile fraction, including carbonates and coatings, was extracted from the suspended matter using cold 0.2 N HCl. This reagent, therefore, releases the total inventory of non-residual trace elements; i.e., those associated with hydrous Fe–Mn oxides, adsorbed on clays, and occurring in carbonates and sulfides in the sediment load (Chester et al., 1985; Elderfield and Sholkovitz, 1987; Tricca, 1997). The residue separated by centrifugation, and the solution was analysed for major and trace elements and Sr isotopic composition. The quantity of acid extractable matter (hereafter referred to as AEM) representing the labile fraction was determined for each sample and expressed as percentage of the total suspended matter content. Uncertainties on the determination of AEM are estimated to be close to $\pm 3\%$.

Table 1
Sampling of the Loire River from May 1995 to March 1996. Results of the river discharge (m^3/s), total suspended matter concentrations (in mg l^{-1}), AEM concentration (%), $\delta^{18}\text{O}$ (‰ vs. PDB) and $\delta^{13}\text{C}$ (‰ vs. PDB), $^{87}\text{Sr}/^{86}\text{Sr}$ ratios and trace-element concentrations (mg/g or $\mu\text{g/g}$)

Sample	Date	W, m^3/s	AEM, %	$\delta^{18}\text{O}$, ‰ vs. PDB	$^{13}\text{C}/\text{PDB}$, ‰ vs. PDB	$^{87}\text{Sr}/^{86}\text{Sr}$	Mn, mg g^{-1}	Ba, mg g^{-1}	Zn, mg g^{-1}	Cu, mg g^{-1}	Sr, $\mu\text{g g}^{-1}$	Ti, $\mu\text{g g}^{-1}$	V, $\mu\text{g g}^{-1}$	Cr, $\mu\text{g g}^{-1}$	Co, $\mu\text{g g}^{-1}$	Ni, $\mu\text{g g}^{-1}$	As, $\mu\text{g g}^{-1}$	Rb, $\mu\text{g g}^{-1}$	Cd, $\mu\text{g g}^{-1}$	Pb, $\mu\text{g g}^{-1}$	Th, $\mu\text{g g}^{-1}$	U, $\mu\text{g g}^{-1}$	Σ REE, $\mu\text{g g}^{-1}$
jlo5	20/05/1995	433	10	-6.4	-5.3	0.710709	8.3	1.54	1.06	0.51	380	142	134	316	48	155	18	21	12	359	1.9	10	720
jlo12	28/05/1995	272	20	-6.7	-3.1	0.711053	3.3	0.67	0.52	0.17	601	70	67	168	19	83	6	17	13	170	0.8	4	268
jlo16	12/06/1995	197	20	-8.3	-7.2	0.711170	4.5	0.76	0.66	0.18	433	60	63	238	15	79	5	16	7	177	1.0	6	242
jlo18	23/06/1995	128	39	-8.6	-7.6	0.711282	1.8	0.39	0.23	0.08	466	25	26	56	6	41	4	8	5	50	0.3	2	99
jlo20	29/06/1995	122	35	-6.7	-6.8	0.711326	1.0	0.37	0.23	0.13	627	19	28	36	5	41	5	15	3	40	0.2	2	79
jlo22	03/07/1995	101	23	-8	-7.6	0.711247	4.9	0.59	0.23	0.85	556	71	85	87	15	102	13	29	4	138	0.6	8	158
jlo25	20/07/1995	91	40	-6.5	-6.1	0.711396	2.3	0.43	0.34	0.23	695	33	25	32	8	65	3	15	2	50	0.2	2	92
jlo26	25/07/1995	71	42	-7	-6.9	0.711306	1.9	0.41	0.30	0.27	656	21	42	20	6	67	4	15	2	70	0.1	3	70
jlo28	03/08/1995	56	38	-9.4	-7.3	0.711258	1.1	0.40	0.53	0.35	619	47	54	27	8	71	8	14	2	73	0.4	5	90
jlo29	11/08/1995	71	46	-9.2	-7.4	0.711265	0.5	0.36	0.30	0.23	613	38	23	18	6	55	6	8	1	53	0.2	2	75
jlo31	18/08/1995	53	43	-8.6	-7.4	0.711297	0.6	0.35	0.36	0.28	596	49	30	14	5	56	9	14	1	45	0.2	3	64
jlo33	27/08/1995	55	41	-9.3	-7.6	0.711224	3.0	0.42	0.51	0.42	598	55	32	26	9	58	15	12	2	77	0.2	2	90
jlo35	05/09/1995	59	35	-9	-7.1	0.711267	1.9	0.37	0.57	0.41	557	44	25	18	5	52	9	17	2	62	0.2	3	75
jlo36	14/09/1995	108	47	-8.5	-7.2	0.711197	2.1	0.41	0.28	0.23	624	43	20	15	6	44	25	9	1	52	0.2	1	71
jlo37	19/09/1995	121	43	-8.7	-7.3	0.711291	2.8	0.51	0.36	0.29	602	63	20	43	9	62	18	9	2	67	0.3	2	104
jlo38	25/09/1995	307	29	-8.8	-7.5	0.711472	4.6	0.77	0.54	0.38	560	66	32	94	18	106	17	12	4	141	0.4	3	192
jlo39	02/10/1995	177	28	-8.2	-7.4	0.711317	6.1	0.83	0.57	0.39	557	81	39	139	20	105	29	13	5	160	0.5	4	212
jlo40	09/10/1995	239	27	-8.1	-7.3	0.711236	5.1	0.87	0.74	0.50	564	113	39	127	20	130	27	17	4	177	0.6	4	234
jlo41	16/10/1995	168	29	-7.6	-7.4	0.711195	5.1	0.83	0.62	0.40	508	145	39	188	19	116	22	19	4	231	0.6	4	226
jlo42	23/10/1995	137	28	-8.1	-7.4	0.711264	5.1	0.80	0.57	0.37	455	257	42	184	21	124	26	25	4	177	1.5	4	210
jlo43	03/11/1995	140	34	-7.4	-7.3	-	3.3	0.60	0.57	0.45	353	258	39	148	32	98	27	5	176	0.6	3	173	
jlo44	27/11/1995	152	24	-4.1	-6.1	0.711253	6.6	0.91	0.55	0.46	605	101	43	250	26	130	46	16	4	198	0.9	4	236
jlo45	03/12/1995	251	14	-6.9	-6.7	0.711084	11.2	1.47	0.99	0.55	488	143	83	252	36	232	34	22	9	438	1.1	7	406
jlo46	12/12/1995	174	15	-6	-7	0.711139	12.7	1.80	1.55	0.94	499	248	107	459	61	298	103	31	9	550	1.3	11	504
jlo47	17/12/1995	165	17	-6.3	-6.7	0.711104	10.9	1.53	1.60	1.21	502	302	98	449	57	247	107	33	8	701	1.1	10	515
jlo48	03/01/1996	760	9	-6.1	-6.9	0.711062	15.9	2.14	1.34	1.08	548	143	129	210	73	261	69	31	12	447	1.6	17	715
jlo49	05/01/1996	935	12	-5.6	-6.7	0.711102	9.8	1.34	0.86	0.36	381	132	96	91	46	146	19	21	9	331	1.5	11	459
jlo50	07/01/1996	920	10	-5.5	-6.2	0.710914	12.0	1.87	1.03	0.38	470	161	136	125	66	176	19	29	11	435	1.7	18	670
jlo51	09/01/1996	965	10	-6.6	-6.4	0.711045	10.3	1.64	0.83	0.35	467	132	112	78	47	140	54	23	9	329	1.2	12	574
jlo52	11/01/1996	830	10	-6.4	-6.4	0.711002	10.7	1.64	1.52	0.59	393	114	99	79	51	138	59	23	9	339	1.1	12	563
jlo53	14/01/1996	1040	9	-7	-6.5	0.710885	12.1	1.74	1.63	1.12	456	125	106	105	63	131	45	23	13	357	1.2	12	593
jlo54	16/01/1996	1050	10	-5.4	-6.2	0.710819	11.3	1.80	1.40	1.38	420	176	115	129	68	151	16	27	9	355	1.2	15	634
jlo55	18/01/1996	830	10	-5.2	-4.8	0.710974	10.0	1.62	0.78	0.33	427	215	113	103	67	129	46	24	9	354	1.4	14	569
jlo56	21/01/1996	620	11	-5.9	-5.3	0.710900	10.4	1.80	0.91	0.36	449	355	115	168	70	194	66	34	10	335	1.8	15	612
jlo57	22/01/1996	560	12	-5.6	-5.6	0.710926	5.5	0.99	0.58	0.26	320	202	82	94	36	87	34	18	7	184	1.0	7	324
jlo58	26/01/1996	525	10	-5.3	-5	0.710986	10.3	1.76	0.86	0.45	455	180	103	183	62	212	45	24	10	309	1.2	12	532
jlo59	29/01/1996	605	11	-5.2	-3.9	0.710590	8.6	1.68	0.67	0.29	468	203	87	112	53	140	22	26	7	272	0.8	14	546
jlo60	01/02/1996	500	10	-4.9	-5.3	0.710769	8.4	1.66	0.76	0.40	540	394	106	215	54	243	38	29	8	287	2.0	13	590
jlo61	06/02/1996	460	11	-4.9	-4.8	0.710830	8.7	1.57	0.84	0.38	410	174	103	219	52	186	39	25	9	334	1.3	12	520
jlo62	12/02/1996	450	11	-4.6	-5.1	0.711000	9.0	1.52	0.83	0.40	431	122	109	164	52	158	41	24	8	332	1.4	12	528
jlo63	15/02/1996	860	8	-4.7	-5.3	0.710382	10.2	1.69	0.69	0.31	480	117	112	89	45	153	28	19	19	270	1.0	9	559
jlo64	19/02/1996	700	8	-5.1	-5.2	0.710985	12.8	2.01	1.02	0.41	390	173	102	154	73	186	51	23	23	390	1.6	15	724
jlo65	22/02/1996	735	9	-4.5	-5.2	0.711020	8.8	1.50	0.67	0.25	331	80	72	103	48	137	26	15	7	287	1.0	10	462
jlo66	27/02/1996	510	10	-1.7	-5.3	0.710839	10.4	1.99	1.03	0.44	462	247	122	250	64	188	85	32	8	436	1.6	12	678
jlo67	08/03/1996	515	10	-3.5	-5.4	0.710896	9.6	1.87	1.44	0.86	427	265	127	152	65	200	62	37	8	451	1.8	16	686
jlo68	18/03/1996	341	11	-4	-4.6	0.710909	8.3	1.68	1.08	0.75	457	229	105	260	58	257	68	31	7	368	1.5	12	604

3.3. Trace-element determination, $^{87}\text{Sr}/^{86}\text{Sr}$ ratio and stable isotope measurements

The concentration of trace elements in the AEM and associated water samples was determined by ICP–MS. The $^{87}\text{Sr}/^{86}\text{Sr}$ ratios were determined using a Finnigan MAT 262 mass spectrometer using standard techniques (Négrel and Grosbois, 1999). The reproducibility of the $^{87}\text{Sr}/^{86}\text{Sr}$ measurements was tested by duplicate analysis of the NBS 987 standard, with a mean value obtained of $0.710227 \pm 17 \cdot 10^{-6}$ (2σ , $n = 70$). The C and O isotopic ratios, reported in per mil deviations from the international PDB standard, were analyzed using a Finnigan MAT 252 mass spectrometer. The average precision, based on multiple analyses of various samples and laboratory standards was $\pm 0.1\%$ for $\delta^{18}\text{O}$ and $\delta^{13}\text{C}$.

4. General features of the suspended matter of the upper Loire catchment

The concentration of suspended matter varied from 3.3 to 100 mg/l, but neither a linear relationship nor a cyclical relationship could be demonstrated between suspended matter concentration and river discharge. This lack of relationship can be explained by the large human impact on the Loire catchment: dredging of the riverbed for gravel extraction and the construction of a large number of dams and reservoirs on the Loire and its tributaries. An XRD semi-quantitative analysis on the suspended matter (Négrel and Grosbois, 1999) has shown that quartz, K-feldspar, plagioclase and calcite represent the main mineral phases, whereas illite and kaolinite are the dominant clay minerals. The contents of quartz and K-feldspar increased with increasing discharge. In contrast, the concentration of calcite varied significantly, from 0% during high flow up to 50% during periods of low flow. The chemistry of the suspended matter was discussed by Négrel and Grosbois (1999).

5. Results

The AEM proportion ranges from 8% to 47% (Table 1) and displays a good relationship with

calcite abundance (Négrel and Grosbois, 1999), reflecting the importance of calcite in the suspended matter. A well-defined relationship is also observed between AEM proportion and Loire River discharge, with the data dispersion falling clearly into two fields (Fig. 2). AEM is highest (45%) at lowest discharge and decreases with discharge from 45% at $5\text{ m}^3/\text{s}$ to 10% at $350\text{ m}^3/\text{s}$ (first field in Fig. 2). AEM is constantly low at about 10% when the river flow exceeds the limit of $350\text{ m}^3/\text{s}$ (second field in Fig. 2).

Tables 1 and 2 summarize data for AEM content of the suspended matter (mass fraction), the trace element and REE concentrations (ppm) of AEM. The concentrations of most trace elements are highest during the high flow period (Fig. 3). The concentrations of the measured trace-element show a wide range with some elements highly concentrated (Table 1), as illustrated by Zn (2.3 mg/g), Cu (1.4 mg/g) or Pb (701 ppm), and fluctuating by a factor of 9 (Zn) to 16 (Cu and Pb). The manganese content ranges from 0.5 to 1.6 mg/g and fluctuates by a factor of 30. Elements considered to be immobile during supergene alteration (Ti, Th) can also have high concentrations in the AEM, as exemplified by Ti which varies from 19 to 394 ppm (a factor of 20) or Th which ranges from 0.1 to 2 ppm (a factor of 14). It is noteworthy that Sr content increases with increasing AEM proportion (Fig. 3).

The total REE contents (ΣREE) in the AEM show large variations (as do individual REE con-

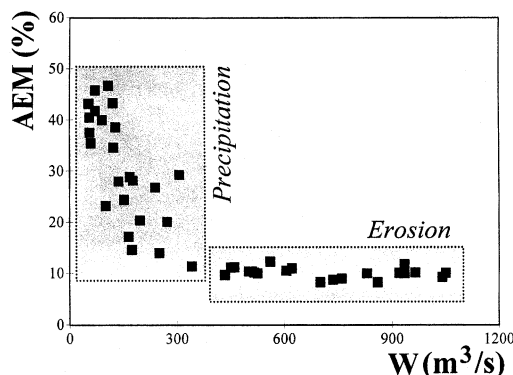


Fig. 2. Relationship between the abundance (%) of AEM in the suspended particulate matter and the discharge of the Loire River ($W/\text{m}^3/\text{s}$); uncertainties $\pm 10\%$.

Table 2

REE systematics in AEM. Elemental REE and Σ REE contents ($\mu\text{g/g}$); $(\text{La}/\text{Yb})_N$ ratio defined by the ratio $\text{La}_{\text{ech}}/\text{Yb}_{\text{ech}}$ to the ratio $\text{La}_{\text{UCC}}/\text{Yb}_{\text{UCC}}$; $(\text{Er}/\text{Nd})_N$ ratio defined by the ratio $\text{Er}_{\text{ech}}/\text{Nd}_{\text{ech}}$ to the ratio $\text{Er}_{\text{UCC}}/\text{Nd}_{\text{UCC}}$. UCC refers to the upper crust composition (Taylor and McLennan, 1985). The cerium and europium anomalies after De Baar et al. (1985) are defined by $\text{Ce}/\text{Ce}^* = 2\text{Ce}_N/[\text{La}_N + \text{Pr}_N]$ and $\text{Eu}/\text{Eu}^* = 2\text{Eu}_N/[\text{Sm}_N + \text{Gd}_N]$. Ce_N , La_N , Pr_N , Eu_N , Sm_N and Gd_N correspond to the UCC normalized concentrations

Sample	La, $\mu\text{g g}^{-1}$	Ce, $\mu\text{g g}^{-1}$	Pr, $\mu\text{g g}^{-1}$	Nd, $\mu\text{g g}^{-1}$	Sm, $\mu\text{g g}^{-1}$	Eu, $\mu\text{g g}^{-1}$	Gd, $\mu\text{g g}^{-1}$	Tb, $\mu\text{g g}^{-1}$	Dy, $\mu\text{g g}^{-1}$	Ho, $\mu\text{g g}^{-1}$	Er, $\mu\text{g g}^{-1}$	Tm, $\mu\text{g g}^{-1}$	Yb, $\mu\text{g g}^{-1}$	Lu, $\mu\text{g g}^{-1}$	(La/ Yb) _N	(Er/ Nd) _N	Ce/ Ce*	Eu/ Eu*
jlo5	137	301	34.7	142	28.9	5.88	25.0	3.45	20.3	3.39	9.30	1.23	7.02	0.97	1.43	0.74	0.99	1.03
jlo12	51.4	108	14.3	53.0	11.9	2.32	9.98	1.32	7.64	1.32	3.35	0.47	2.54	0.35	1.48	0.71	0.91	1.00
jlo16	47.3	96.6	13.4	49.1	8.59	1.90	8.83	1.38	7.31	1.34	3.01	0.45	2.34	0.35	1.48	0.69	0.87	1.02
jlo18	19.3	40.7	4.63	19.7	3.89	0.84	3.39	0.51	2.59	0.53	1.27	0.18	0.96	0.14	1.47	0.73	0.98	1.09
jlo20	15.5	33.2	3.58	15.2	2.93	0.65	2.79	0.40	2.03	0.41	0.99	0.14	0.74	0.11	1.54	0.74	1.02	1.07
jlo22	29.5	68.9	7.35	30.3	6.04	1.32	5.20	0.75	3.91	0.77	1.83	0.28	1.46	0.21	1.48	0.68	1.07	1.11
jlo25	18.0	40.4	4.16	16.7	3.41	0.76	2.98	0.43	2.20	0.45	1.09	0.16	0.73	0.11	1.81	0.74	1.06	1.12
jlo26	13.4	30.7	3.10	13.1	2.54	0.53	2.30	0.33	1.79	0.34	0.86	0.13	0.61	0.09	1.61	0.74	1.09	1.03
jlo28	16.9	40.0	4.02	16.7	3.32	0.76	3.01	0.44	2.41	0.50	1.17	0.18	0.88	0.13	1.41	0.79	1.11	1.13
jlo29	14.2	32.8	3.31	13.8	2.81	0.62	2.45	0.35	1.94	0.39	0.97	0.15	0.74	0.10	1.41	0.79	1.09	1.11
jlo31	12.1	28.3	2.82	12.1	2.42	0.53	2.14	0.34	1.62	0.35	0.85	0.13	0.67	0.09	1.32	0.79	1.10	1.09
jlo33	17.2	39.4	3.99	16.9	3.29	0.76	2.91	0.43	2.29	0.45	1.18	0.16	0.87	0.13	1.45	0.79	1.08	1.15
jlo35	14.3	33.2	3.35	14.0	2.74	0.63	2.47	0.36	1.91	0.37	0.93	0.14	0.75	0.11	1.40	0.75	1.09	1.14
jlo36	13.5	31.3	3.15	13.5	2.64	0.58	2.37	0.33	1.74	0.35	0.83	0.12	0.70	0.09	1.41	0.70	1.09	1.09
jlo37	19.9	45.7	4.61	19.4	3.93	0.87	3.61	0.51	2.60	0.51	1.19	0.18	0.97	0.13	1.50	0.69	1.09	1.08
jlo38	35.8	83.5	8.97	36.8	7.17	1.61	6.44	0.90	4.81	0.94	2.24	0.34	1.74	0.24	1.51	0.69	1.06	1.11
jlo39	40.5	92.1	9.89	40.3	8.00	1.78	7.15	1.00	5.25	1.03	2.52	0.37	1.96	0.27	1.52	0.71	1.05	1.11
jlo40	44.3	101	11.5	44.6	8.76	1.94	8.03	1.08	5.97	1.11	2.79	0.39	2.19	0.30	1.48	0.71	1.02	1.09
jlo41	42.4	98.2	11.0	42.8	8.87	1.94	7.69	1.06	5.60	1.05	2.67	0.39	2.06	0.29	1.51	0.71	1.04	1.10
jlo42	41.5	89.1	11.2	39.1	7.79	1.70	6.76	1.03	5.16	1.01	2.51	0.37	2.03	0.33	1.50	0.73	0.94	1.10
jlo43	33.9	73.5	9.07	33.1	6.28	1.37	5.41	0.84	4.64	0.74	1.87	0.24	1.60	0.22	1.55	0.64	0.95	1.10

jlo44	46.2	102	11.2	45.4	8.46	1.98	7.34	1.06	5.83	1.17	2.73	0.41	2.30	0.27	1.47	0.68	1.02	1.18
jlo45	80.3	171	19.5	77.7	15.9	3.25	14.0	1.87	10.7	1.89	4.98	0.67	3.79	0.51	1.55	0.72	0.99	1.02
jlo46	97.6	216	23.9	95.8	19.0	4.42	16.5	2.60	13.3	2.58	6.12	0.92	4.84	0.65	1.48	0.72	1.02	1.17
jlo47	104	206	23.7	117	17.2	3.83	15.6	2.27	12.3	2.24	5.37	0.79	4.29	0.61	1.78	0.52	0.95	1.10
jlo48	136	313	33.1	133	26.7	6.04	22.8	3.48	18.5	3.67	8.88	1.37	6.96	1.03	1.43	0.75	1.06	1.15
jlo49	86.7	201	20.9	86.7	17.3	3.77	15.2	2.20	11.4	2.33	5.78	0.85	4.31	0.64	1.48	0.75	1.08	1.09
jlo50	130	296	29.8	122	25.0	5.36	22.1	3.31	16.8	3.50	8.03	1.20	6.07	0.89	1.57	0.74	1.08	1.07
jlo51	110	256	26.4	102	20.9	4.34	19.3	2.93	14.8	3.08	7.03	1.10	5.03	0.71	1.60	0.78	1.08	1.01
jlo52	108	246	26.0	103	20.4	4.84	19.6	2.90	14.7	2.81	7.32	0.92	5.52	0.75	1.43	0.80	1.06	1.14
jlo53	113	257	27.6	111	22.2	5.01	20.6	3.04	15.9	3.24	7.18	1.06	5.63	0.85	1.47	0.73	1.05	1.10
jlo54	123	276	30.4	116	22.4	5.83	20.7	3.10	17.0	3.37	7.81	1.12	6.05	0.79	1.49	0.76	1.03	1.27
jlo55	114	251	26.3	99.6	20.5	4.85	18.5	2.93	14.4	2.86	6.66	1.09	5.13	0.79	1.63	0.76	1.05	1.17
jlo56	123	268	28.5	106	22.3	5.52	20.6	2.97	15.9	3.37	7.34	1.17	6.25	0.91	1.44	0.76	1.03	1.21
jlo57	65.8	141	15.3	57.0	11.6	3.14	11.2	1.51	8.11	1.65	3.90	0.57	3.14	0.47	1.54	0.77	1.01	1.29
jlo58	109	227	25.4	93.3	19.9	4.77	18.4	2.80	14.9	2.85	6.78	1.02	5.36	0.86	1.49	0.82	0.98	1.17
jlo59	116	234	26.0	94.2	20.1	4.50	17.7	2.84	14.3	2.82	6.48	0.99	5.50	0.73	1.55	0.78	0.97	1.12
jlo60	121	256	27.5	104	21.1	5.12	19.2	2.84	14.8	2.92	7.59	1.09	6.08	0.76	1.46	0.83	1.01	1.19
jlo61	102	224	24.9	94.0	19.6	4.21	17.4	2.66	15.1	2.76	6.39	0.92	5.36	0.73	1.40	0.77	1.01	1.07
jlo62	103	228	24.6	96.4	21.1	4.37	18.7	2.61	13.7	2.73	6.19	0.88	4.86	0.73	1.55	0.73	1.03	1.03
jlo63	111	239	26.7	101	21.1	4.79	19.9	2.86	15.0	3.08	7.40	1.12	5.68	0.81	1.43	0.83	1.00	1.10
jlo64	140	311	33.9	133	28.6	6.02	25.8	3.84	19.5	4.02	9.00	1.43	7.05	1.00	1.46	0.76	1.03	1.04
jlo65	90.0	197	21.9	85.3	16.9	4.00	16.6	2.61	13.0	2.71	5.92	0.85	4.83	0.66	1.37	0.78	1.01	1.12
jlo66	134	288	32.4	125	26.3	5.74	23.5	3.48	17.9	3.65	8.52	1.19	6.80	1.05	1.45	0.77	1.00	1.08
jlo67	139	291	32.8	128	25.3	5.99	23.0	3.43	17.1	3.59	8.18	1.25	6.79	0.98	1.50	0.72	0.98	1.17
jlo68	122	253	28.8	116	22.7	5.31	19.6	2.93	15.8	3.06	7.30	1.10	5.69	0.88	1.57	0.71	0.97	1.18

tents) from 64 to 720 ppm and are inversely correlated with the AEM concentration (Fig. 3). The REE concentrations are presented in Fig. 4 as upper conti-

mental crust normalized patterns (UCC data from Taylor and Mc Lennan, 1985). The normalized REE patterns for the AEM are nearly flat with a $(La/Yb)_N$

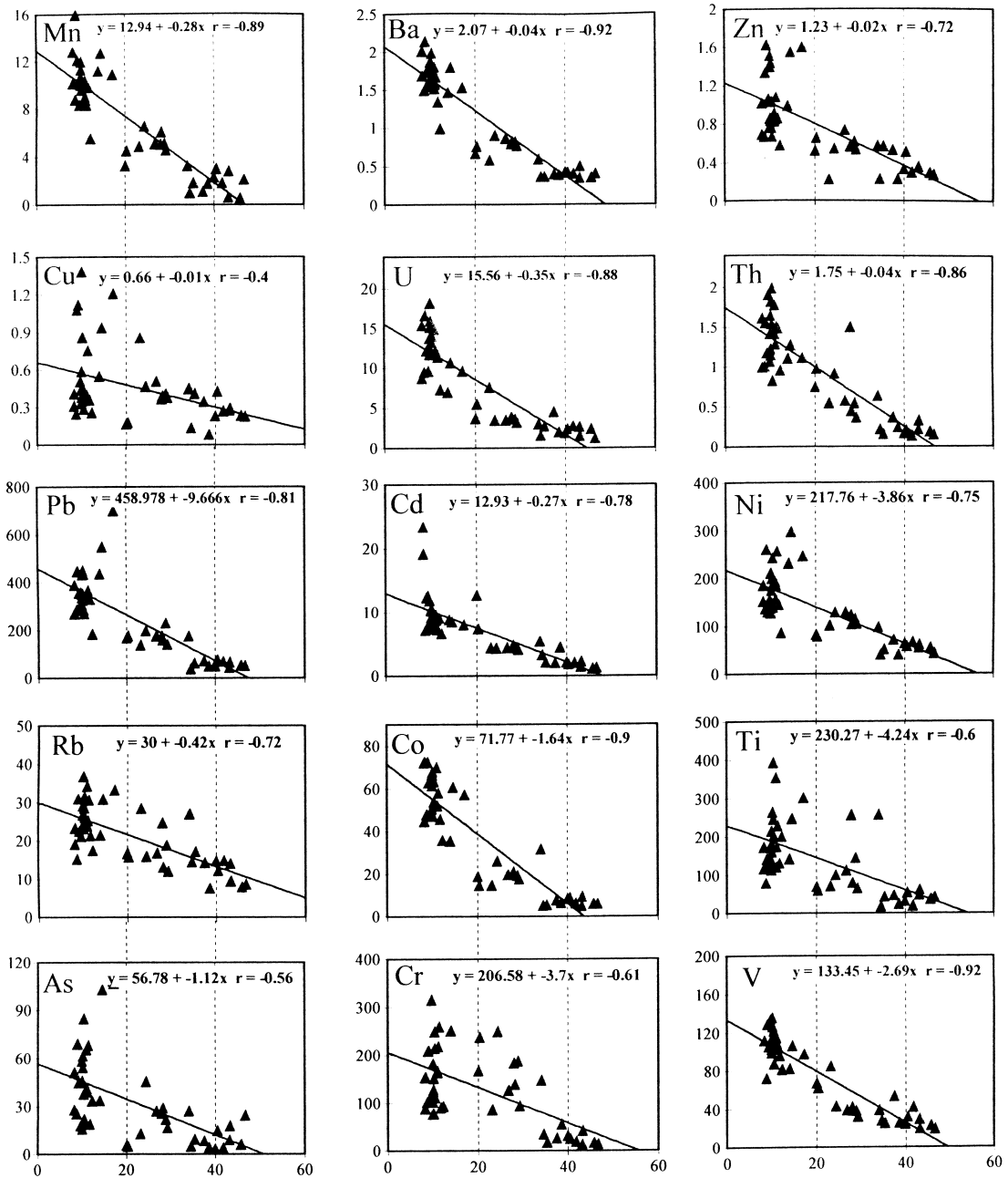


Fig. 3. Plot of elemental concentration (in ppm) vs. the percentage of AEM in the suspended particulate matter of the Loire River. Elements are arranged according to dispersion.

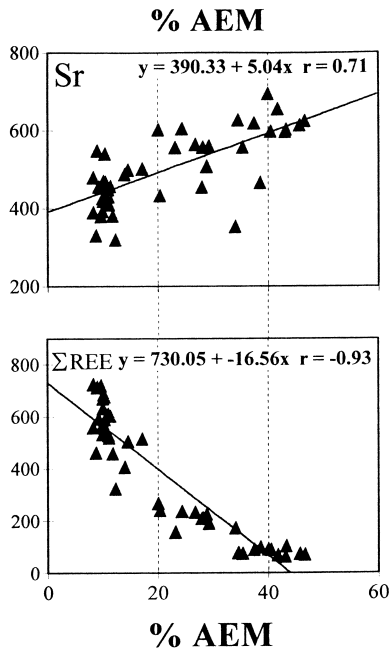


Fig. 3 (continued).

ratio in the range 1.3–1.8 which indicates a slight enrichment in light REE (LREE) compared to heavy REE (HREE) and is in agreement with the $(Er/Nd)_N$

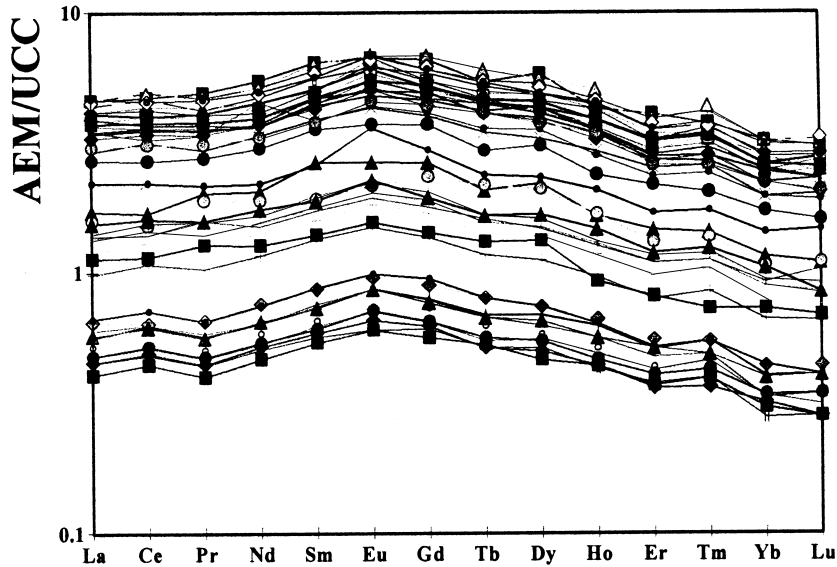


Fig. 4. UCC normalized patterns for REE in AEM in the suspended particulate matter of the Loire River.

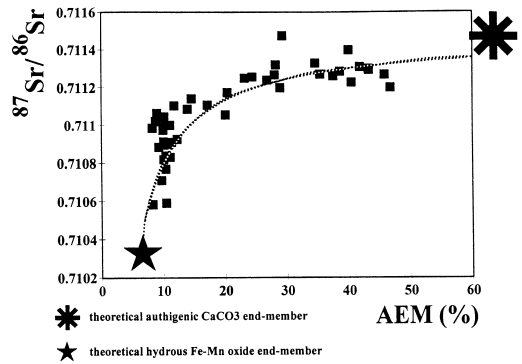


Fig. 5. $^{87}Sr/^{86}Sr$ ratios plotted against the abundance (%) of AEM in the suspended particulate matter of the Loire River. The curve represents the calculated mixing line which relies the theoretical authigenic carbonate end-member to the theoretical hydrous Fe–Mn oxides one.

ratios, which range from 0.63 to 0.82. However, there is no relationship between these ratios and the discharge of the river or AEM concentration. Two of the REEs (Eu and Ce) may develop anomalies due to differences in their oxidation states relative to the other REE. The most stable oxidation state of most of the REEs is 3+, but under oxidizing and reducing conditions, respectively, Ce^{4+} and Eu^{2+} may

become significant. In AEM, only Eu/Eu^* shows a slight deviation from unity (1.11 ± 0.06), reflecting a terrestrial source as shown by Nath et al. (1997).

The $^{87}\text{Sr}/^{86}\text{Sr}$ ratio in the AEM varies significantly from 0.710582 to 0.711472 (Table 1) with two different trends when plotted against AEM concentration (Fig. 5). The first trend is an increase in the $^{87}\text{Sr}/^{86}\text{Sr}$ ratio from 0.71058 to around 0.7111, corresponding to the low abundance of AEM, whereas the second trend is a slight increase in the $^{87}\text{Sr}/^{86}\text{Sr}$ ratio (0.7111 to 0.71147) corresponding to the period when AEM proportion increase. The carbonate fraction of the suspended matter in the Loire

River was analysed for the C and O stable isotopes during a complete hydrological cycle. The recorded values vary from -3.1‰ to -7.6‰ for $\delta^{13}\text{C}$ and from -1.7‰ to -9.4‰ for $\delta^{18}\text{O}$. The relationship between $\delta^{18}\text{O}$ and $\delta^{13}\text{C}$ (Fig. 6) indicates that “winter” carbonates sampled during high-flow conditions ($W > 350 \text{ m}^3/\text{s}$) are clearly separated from “summer” carbonates sampled during low-flow conditions ($W < 350 \text{ m}^3/\text{s}$). The latter occupy a restricted area with $\delta^{13}\text{C} = -7\text{‰}$ (PDB) and $\delta^{18}\text{O} = -8\text{‰}$ (PDB). Winter carbonates are enriched in both ^{13}C and ^{18}O by approximately 2‰ at times of the minimum AEM concentration.

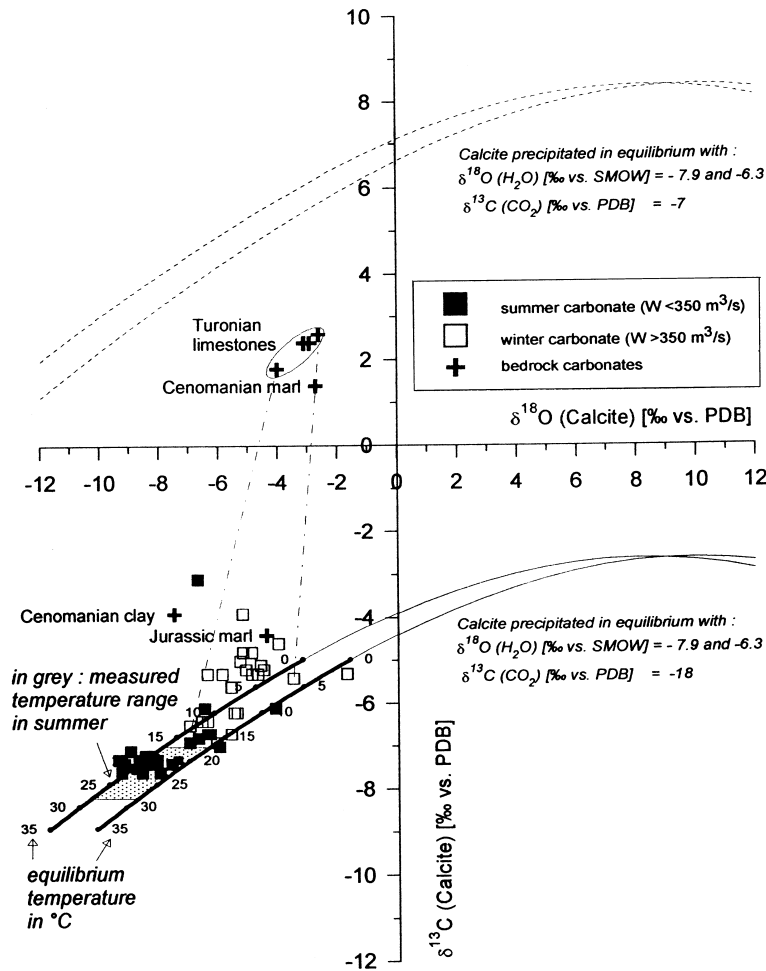


Fig. 6. Plot of $\delta^{18}\text{O}$ (‰ PDB) vs. $\delta^{13}\text{C}$ (‰ PDB) for the carbonate fraction of suspended particulate matter of the Loire River.

6. Discussion

One of the main features in the labile fraction of suspended material carried by the Loire River during its hydrological cycle is the existence of two different fields when the proportion of AEM is plotted vs. the discharge of the river (Fig. 2). These two fields correspond to time-related processes within the river and thus reflect two end-member inputs.

The first field can be related to the period of the hydrologic cycle when CaCO_3 precipitation is dominant (Négrel and Grosbois, 1999), i.e., during low flow in summer. This agrees with the work of Roy et al., (1998) on the Seine river. During the summer months, water is saturated to oversaturated with respect to calcite (Grosbois, 1999), and XRD analyses confirm large amounts of calcite. Discharge exceeding the level of 350 m/s, erosion becomes the dominant source of suspended matter. This is indicated by the high contents of K-feldspar and plagioclase in the suspended matter. However, the leaching by cold HCl cannot release elements from these minerals and the high trace element concentrations in suspended matter during high flow are bound to hydrous Fe–Mn oxides or adsorbed onto clays.

An important feature of the REE patterns is the evidence of a middle REE (MREE) enrichment over the LREE and HREE (Fig. 4). In river systems, Fe–Mn coatings on silicate particles (Sposito, 1989; Robinson, 1993) and on suspended matter (Rhine — Tricca, 1997; Shine et al., 1995) have been recognized as efficient carriers of REE with an MREE-enriched pattern (Granjean-Lecuyer et al., 1993; Sholkovitz, 1995; Tricca, 1997). This link between REE and Fe–Mn coatings is also supported by a positive relationship between ΣREE and Mn concentrations as found by Tricca (1997) from suspended matter in the Rhine river. MREE-enriched patterns have been recognized in a large variety of terrestrial waters (river waters — Sholkovitz, 1995; Gaillardet et al., 1997; acidic waters — Johannesson et al., 1996) and in acid leachates of rocks or minerals (metasedimentary rocks, sandstones, apatites, etc.) by several workers (Gosselin et al., 1992; Granjean-Lecuyer et al., 1993; Schaltegger et al., 1994; Zhou et al., 1995).

In our data, the ΣREE are inversely correlated with the calcite fraction in the suspended matter. As

AEM concentrations increase, a large decrease in ΣREE concentrations is observed (Fig. 3) with a correlation coefficient of $r = -0.93$. Moreover, the ΣREE are positively correlated with Mn and negatively correlated with Sr, as defined by the following relationships: $\text{Mn} = 0.053 \Sigma\text{REE} + 3.30$ ($r = 0.92$) and $\Sigma\text{REE} = -1.607\text{Sr} + 1177.1$ ($r = 0.64$). Bellanca et al. (1997) studied such phenomena in a stratigraphic succession from Albian to Cenomanian and demonstrated a strong negative correlation between the ΣREE and CaO. Marine carbonate phases are well known to be poor in REE in comparison to detrital clays and heavy minerals (Piper, 1974). We conclude from the REE data that:

1. Fe–Mn coatings on silicate particles are the principal trace element carrying phase,
2. the fluctuations of ΣREE and AEM concentrations are due to a “dilution” of a terrigenous component (i.e., Fe–Mn coatings) by calcite precipitation during low flow.

The variation of $^{87}\text{Sr}/^{86}\text{Sr}$ ratios in the AEM reflects the mixing of strontium co-precipitated with hydrous Fe–Mn oxides, adsorbed on clays, and bound in carbonates. The strong variation of the $^{87}\text{Sr}/^{86}\text{Sr}$ ratios from 0.71058 to around 0.7111 at nearly constant AEM corresponds to the erosion-dominated period (Fig. 5). The trend with a weak increase in the $^{87}\text{Sr}/^{86}\text{Sr}$ ratio (0.7111 to 0.71147) with AEM corresponds to the period when flow rates are low and neoformation of calcite occurs. The relationship between the $^{87}\text{Sr}/^{86}\text{Sr}$ ratio and AEM concentration reflects variations in the contributions of the two main end-members, i.e., the hydrous Fe–Mn oxides with the lower $^{87}\text{Sr}/^{86}\text{Sr}$ ratio (≈ 0.7105) and the carbonates with the higher $^{87}\text{Sr}/^{86}\text{Sr}$ ratio (≈ 0.7115). The removal of dissolved Sr both by oxides and by carbonates, as suggested by Fig. 3 and as demonstrated by Casanova et al. (1999), implies that the $^{87}\text{Sr}/^{86}\text{Sr}$ ratio cannot be directly compared to the Sr content in mixing diagrams (Faure, 1986). We calculated the mixing line between the $^{87}\text{Sr}/^{86}\text{Sr}$ ratio and AEM (Fig. 5) between the two end-members in order to better constrain the data. A representative mixing line relies the theoretical authigenic carbonate end-member ([AEM] = 100%, $^{87}\text{Sr}/^{86}\text{Sr} = 0.7116$) to the theoretical hydrous Fe–Mn oxides

one ($[AEM] = 6\%$, $^{87}\text{Sr}/^{86}\text{Sr} = 0.7105$). This evolutionary pathway is likely to reflect the simple binary mixing between the two end-members.

However, the fact, that, in general, hydroxides and carbonates are in isotopic equilibrium with the water phase (Casanova et al., 1999) implies that the strontium isotopic composition of carbonates and iron oxides formed in continental environments can be used as tracer of the water in which they formed. The highest $^{87}\text{Sr}/^{86}\text{Sr}$ ratios, close to the carbonate end-member are identical to the mean value of dissolved Sr during low flow (0.711432 ± 0.0002 ($n = 23$, Grosbois et al., in press).

The low Sr ratios in AEM measured during high flow (≈ 0.7105) differ clearly from those of the dissolved load during the same period at the AEM sampling point (0.71158 ± 0.0001 , $n = 21$; Grosbois et al., in press). The isotopic signature of hydroxides should reflect that of the water from which they formed. Waters with such low $^{87}\text{Sr}/^{86}\text{Sr}$ ratios can be found in rivers draining the Massif Central. Négrel et al. (1997) report a range 0.709511 (low water) to 0.712656 (high water) for the Allier river.

It is, therefore, suggested that the oxides may originate from the Massif Central and are transported by the Allier and the Loire to the sampling point. The observed difference between the $^{87}\text{Sr}/^{86}\text{Sr}$ ratio of oxides and that of the waters during high flow implies a conservative behaviour of the Sr isotopic signature within the oxides. Oxides seem not to be re-equilibrated with the waters during transport.

Further constraints on the origin of the carbonate fraction in the suspended matter can be obtained by an examination of the stable isotope systematics of the carbonates. The isotopic composition of the summer carbonates can be explained by calcite precipitation in isotopic equilibrium with the river water (the measured $\delta^{18}\text{O}$ range in the Loire River is between -6.3% and -7.9% vs. SMOW) and dissolved CO_2 , which is characterized by a $\delta^{13}\text{C}$ of -18% (PDB). Fig. 6 shows the curves for calcite precipitation and the corresponding equilibrium temperatures based on the classical equations for carbonate-water isotopic exchange of Craig (1965) for $\delta^{18}\text{O}_{\text{carb}} = f(tC)$ and Bottinga (1968) for $\delta^{13}\text{C}_{\text{carb}} = f(tC)$. In the latter case, the approximation of Fontes et al., (1973) was used (see also Dever et al., 1983). Most of the summer carbonates may have precipitated

within the range of measured water temperatures of $17\text{--}28^\circ\text{C}$.

The presumed $\delta^{13}\text{C}$ value of -18% (PDB) is comparable to a $\delta^{13}\text{C}$ of -8.5% of TDIC measured in one Loire water sample collected in July if we take into account the enrichment factor $\epsilon(\text{CO}_{2\text{g}} - \text{HCO}_3^-)$ of approximately 9% at 17°C (Mook et al., 1974). Consequently, the isotopic composition of the CO_2 implied in the formation of authigenic calcite in the Loire River during low-water conditions represents an intermediate isotopic composition derived from mixing between plant-derived ($\delta^{13}\text{C} < -25\%$) and atmospheric (-7%) CO_2 . Assuming a biogenic CO_2 isotopic composition of -28% , both sources contribute about 50% of TDIC in proportions that vary only slightly during the low-flow period. The isotopic enrichment of the ‘‘winter’’ carbonates may reflect different processes.

(1) Precipitation of authigenic calcite at lower temperatures. Even high-flow samples are saturated with respect to calcite (Grosbois et al., in press) and plot within the equilibrium curves for $\delta^{13}\text{C}(\text{CO}_2) = -28\%$ on Fig. 6.

(2) Authigenic calcite formation from CO_2 with a larger component of atmospheric CO_2 relative to biogenic CO_2 (the equilibrium curves for $\delta^{13}\text{C}(\text{CO}_2) = -7\%$ are plotted as dashed lines in Fig. 6).

(3) Mixing of authigenic calcite precipitated at low temperatures with detrital calcite derived from the erosion of isotopically enriched marine carbonate rocks cropping out in the Middle Loire watershed. Six representative rock samples were analysed for their stable isotope contents (Table 3). The samples include Jurassic marl and limestone, Cenomanian

Table 3
 $\delta^{18}\text{O}$ (‰ vs. PDB) and $\delta^{13}\text{C}$ (‰ vs. PDB) of selected basements from the Loire catchment

Sample	Type	$\delta^{18}\text{O}$, ‰ vs. PDB	$\delta^{13}\text{C}$, ‰ vs. PDB
1	limestone (Turonian)	-2.6	2.6
8	chalk (Turonian)	-2.9	2.4
10	limestone (Jurassic)	-4	1.8
17	marl (Cenomanian)	-2.7	1.4
20	argillaceous sand (Cenomanian)	-7.5	-3.9
28	marl (Jurassic)	-4.4	-4.4
30	chalk (Turonian)	-3.1	2.4

marl and argillaceous sand, chalk and other limestones of Turonian age. Except for two samples, the $\delta^{18}\text{O}$ and $\delta^{13}\text{C}$ contents fall in the typical range of marine carbonates. Fig. 6 shows the representative points and potential mixing lines between detrital calcite and low-temperature authigenic calcite.

(4) Some contribution of eroded soil-derived carbonate material (secondary calcite with a lighter isotopic signature) to the suspended carbonate fraction during high-flow conditions cannot be excluded.

7. Synthesis and perspectives

By combining trace element and REE analysis of the AEM in the suspended matter of the middle Loire River with Sr, C and O isotope data obtained for AEM, the dissolved phase and rocks of the drainage basin, our study comes to the following conclusions on the origin and the transport mechanisms of trace metals in the Loire drainage basin.

(1) During high flow conditions, AEM is mainly provided by erosion, during low flow calcite neof ormation becomes dominant.

(2) Only erosion-derived AEM contributes significantly to the global trace metal transport. During low flow, the erosive fraction is “diluted” by calcites poor in trace elements.

(3) REE patterns reveal the nature of the solid phase carrying trace elements: Fe and Mn hydroxide coatings on particles are the most probable candidate.

(4) Sr isotopes give indications on the geographical distribution of the trace element sources. Sr integrated into neof ormed calcites is directly derived from the local dissolved load. Fe and Mn hydroxides may have precipitated in waters similar to those found in the upstream part of the basin (crystalline basement of the Massif Central).

(5) The Sr isotope signal of hydroxides is conservative, i.e., hydroxides do not re-equilibrate with downstream water.

(6) Calcite precipitation during low flow takes place in isotopic equilibrium with local stream water and biogenic CO_2 . During high flow, the proportion of atmospheric CO_2 and/or of erosive carbonates increases.

Future research will have to focus on the upstream part of the drainage basin and investigate the nature and origin of the Fe–Mn coatings and their capacity of transport of chemical species, pollutants like Pb, Zn, As and Cu as well as typical crustal tracers as Th, Ti and Rb.

On the other hand, the findings in the central part of the basin may have important implications for investigations of the output into the estuary. In this zone, Fe and some other trace elements are controlled by the adsorption onto Fe-hydroxides formed in situ (Négrel, 1997). The fate of the two components of AEM under the highly variable chemical conditions of the estuary will constitute a second axis of research focused on trace element mobility and water quality preservation in coastal areas.

Once the present day mechanisms (including biological triggering of calcite and hydroxide precipitation, Grosbois et al. in press) of trace metal transport are elucidated, reconstruction of previous steps in the evolution of the basin may become possible. Ongoing studies focus on the distribution of trace elements in the labile fraction of sediment cores from the Middle Loire alluvial plain covering a period of time from 0 to 10000 yr B.P. (Garcin et al., 1999). This study should allow improving the knowledge of the functioning of the catchment with regard to anthropogenic and pre-anthropogenic history.

Acknowledgements

This work was supported by the BRGM (Bureau de Recherche Géologiques et Minières) research program “PRR203, Morphogénèse Fluviale”. The authors would like to thank Michel Brach for his technical assistance in the physico-chemical analyses and sampling, and the TIMS team (led by C. Guerrot) and the ICP–MS team (led by A. Cocherie) for rapid analyses. Thanks are also extended to Joël Casanova and Philippe Baranger for their helpful comments. The authors gratefully acknowledge Dr. Dalila Ben Othmann, Prof. J.I. Drever and an anonymous reviewer for significant improvements of the manuscript. Patrick Skipwith is thanked for improving the English. This is BRGM contribution no. 99007. [JD]

References

- Albarède, F., Semhi, K., 1995. Patterns of elemental transport in the bedload of the Meurthe River (NE France). *Chem. Geol.* 122, 129–145.
- Bellanca, A., Masetti, D., Nri, R., 1997. REE in limestone/marls couplets from the Albian–Cenomanian Cismon section (Venetian Region, northern Italy): assessing REE sensitivity to environmental changes. *Chem. Geol.* 141, 141–152.
- Bottinga, Y., 1968. Calculation of fractionation factors for carbon and oxygen isotopic exchange in the system calcite–carbon dioxide–water. *J. Phys. Chem.* 72 (3), 800–807.
- Breward, N., Williams, M., Bradley, D., 1996. Comparison of alternative extraction methods for determining particulate metal fractionation in carbonate-rich Mediterranean soils. *Appl. Geochem.* 11, 101–104.
- BRGM, 1996. Carte Géologique de la France au 1/1.000.000. 6th edn.
- Casanova, J., Bodéan, F., Négrel, Ph., Azaroual, M., 1999. Microbial control on the precipitation of ferrihydrite and carbonate modern deposits from the Cézallier hydrothermal springs Massif Central, France). *J. Sediment. Geol.* 126, 125–145.
- Chester, R., Kudoja, W.M., Thomas, A., Towner, J., 1985. Pollution reconnaissance in stream sediments using non-residual trace metals. *Environ. Pollut.* 10, 213–238.
- Craig, H., 1965. The measurement of oxygen isotope paleotemperatures. In: Tongiorgi, E. (Ed.), *Stable isotopes in oceanographic studies and paleotemperatures*. Proc. Spoleto Conference, Pisa. pp. 3–24.
- De Baar, H.J.W., Bacon, M.P., Brewer, P.G., Bruland, K.W., 1985. Rare earth elements in the Atlantic and Pacific Oceans. *Geochim. Cosmochim. Acta* 49, 1943–1959.
- Dever, L., Durand, R., Fontes, J.C.H., Vachier, P., 1983. Etude Pédogénétique et Isotopique des Néofonnations de Calcite Dans un sol sur Craie, Caractéristiques et Origine. *Geochim. Cosmochim. Acta* 47, 2079–2090.
- Elderfield, H., Sholkovitz, E.R., 1987. REE in the pore-waters of reducing nearshore sediments. *Earth Planet. Sci. Lett.* 82, 280–288.
- Faure, G., 1986. *Principles of Isotope Geology*. Wiley, 588 pp.
- Figueres, G., Martin, J.M., Meybeck, M., Seyler, P., 1985. A comparative study of mercury contamination in the Tagus estuary (Portugal) and major French estuaries (Gironde Loire, Rhône). *Estuarine, Coastal Shelf Sci.* 20, 183–203.
- Fontes, J.C.H., Lepvrier, C., Melières, F., Pierre, C., 1973. Isotopes Stables dans les Carbonates Évaporitiques du Miocène Supérieur de Méditerranée Occidentale. In: *Messinian Events in the Mediterranean*. Koninklijke Nederlandse Akademie van Wetenschappen, Amsterdam, pp. 91–100.
- Gaillardet, J., Dupré, B., Allègre, C.J., Négrel, Ph., 1997. Chemical and physical denudation in the Amazon River basin. *Chem. Geol.* 142, 141–173.
- Garcin, M., Giot, D., Farjanel, G., Gourry, J.-C., Kloppmann, W., Négrel, Ph., 1999. Géométrie et Âge du Remplissage Holocène de la Loire Moyenne, Exemple du Val d'Avary (France, Loire et Cher). *C. R. Acad. Sci.* 329, 405–412.
- Gosselin, D.G., Smith, M.R., Lepel, E.A., Laul, J.C., 1992. REE in chloride rich groundwater Palo-Duro Basin, Texas, USA. *Geochim. Cosmochim. Acta* 56, 1495–1505.
- Granjean-Lecuyer, P., Feist, R., Albarède, F., 1993. REE in old biogenic apatites. *Geochim. Cosmochim. Acta* 57, 2507–2514.
- Grosbois, C., 1999. *Géochimie des eaux de la Loire: contributions naturelles et anthropiques, Quantification de l'érosion*. PhD Thesis, Univ. Tours, 232 pp.
- Grosbois, C., Négrel, P., Fouillac, C., Grimaud, D., in press. Chemical and isotopic characterization of the dissolved load of the Loire river. *Chem. Geol.*
- Johannesson, K.H., Lyons, W.B., Yelken, M.A., Gaudette, H.E., Stetzenbach, K.J., 1996. Geochemistry of the rare earth elements in hypersaline and dilute acidic natural terrestrial waters: complexation behavior and middle rare earth element enrichments. *Chem. Geol.* 133, 125–144.
- Leleyter, L., Probst, J.L., 1998. Partitioning of trace elements in different world river sediments by chemical extraction technique. In: *Abstract Goldschmidt Conference*, Toulouse. *Mineral. Mag.* Vol. 62Ap. 879.
- Meade, R.H., Yuzyk, T.R., Day, T.J., 1990. Movement and storage of sediment in rivers of the United States and Canada. In: *Surface Water Hydrology Vol. O-1 Geological Society of America*, pp. 255–280.
- Milliman, J.D., Meade, R.H., 1983. World-wide delivery of river sediment to the oceans. *J. Geol.* 91, 1–21.
- Mook, W.G., Bommerson, J.C., Staverman, W.H., 1974. Carbon isotope fractionation between dissolved bicarbonate and gaseous carbon dioxide. *Earth Planet. Sci. Lett.* 22, 169–176.
- Nath, B.N., Bau, M., Ramalingeswara Rao, B., Rao, C.M., 1997. Trace and rare earth elemental variation in Arabian Sea sediments through a transect across the oxygen minimum zone. *Geochim. Cosmochim. Acta* 61, 2375–2388.
- Négrel, Ph., 1997. Multi-elements chemistry of Loire estuary sediments: anthropogenic versus natural sources. *Estuarine, Coastal Shelf Sci.* 44, 395–411.
- Négrel, Ph., Deschamps, P., 1996. Natural and anthropogenic budgets of small watershed in the Massif central (France): chemical and strontium characterization of water and sediments. *Aquat. Geochem.* 2, 1–27.
- Négrel, Ph., Fouillac, C., Brach, M., 1997. Occurrence of mineral water springs in the stream channel of the Allier River (Massif Central, France): chemical and Sr isotope constraints. *J. Hydrol.* 203, 143–153.
- Négrel, Ph., Grosbois, C., 1999. Changes in distribution patterns of chemical elements and $^{87}\text{Sr}/^{86}\text{Sr}$ isotopic signatures in suspended matter and bed sediments transported out by the upper Loire River watershed (France). *Chem. Geol.* 156, 213–249.
- Piper, D.Z., 1974. REE in the sedimentary cycle: a summary. *Chem. Geol.* 14, 285–304.
- Prohic, E., Juracic, M., 1989. Heavy metals in sediments — problems concerning determination of the anthropogenic influence. Study in the Krka River Estuary, Eastern Adriatic Coast Yugoslavia. *Environ. Geol. Water Sci.* 13, 145–151.
- Robinson, G.D., 1993. Major element chemistry and micromorphology of Mn-oxides coatings on stream alluvium. *Appl. Geochem.* 8, 633–642.

- Roy, S., Gaillardet, J., Allégre, C.J., 1998. Geochemistry of dissolved and suspended loads of the Seine river, France: anthropogenic impacts, carbonate and silicate weathering. *Geochim. Cosmochim. Acta* 63, 1277–1292.
- Schaltegger, U., Stille, P., Rais, N., Pique, A., Clauer, N., 1994. Nd and Sr isotopic dating of diagenesis and low grade metamorphism of argillaceous sediments. *Geochim. Cosmochim. Acta* 58, 1471–1481.
- Shine, J.P., Ika, R.V., Ford, T.E., 1995. Multi-variate statistical examination of spatial and temporal patterns of heavy metals contamination in New Bedford Harbor marine sediments. *Environ. Sci. Technol.* 29, 1781–1788.
- Sholkovitz, E.R., 1989. Artifacts associated with the chemical leaching of sediments for REE. *Chem. Geol.* 77, 47–51.
- Sholkovitz, E.R., 1995. The aquatic geochemistry of the rare earth elements in rivers and estuaries. *Aquat. Geochem.* 1, 1–43.
- Sposito, G., 1989. *The Chemistry of Soils*. Oxford University Press, 277 pp.
- Taylor, S.R., Mc Lennan, S.M., 1985. *The Continental Crust: its Composition and Evolution*. Blackwell Scientific Publications, 312 pp.
- Tessier, A., Campbell, P.G.C., Bisson, M., 1979. Sequential extraction procedure for the speciation of particulate trace metals. *Anal. Chem.* 51 (7), 844–851.
- Tricca, A., 1997. Transport mechanisms of trace elements in surface and groundwater: Sr, Nd, U and rare earth elements evidence. PhD Thesis, University of Strasbourg, 234 pp.
- Zhou, X., Johannesson, K.H., Stetzenbach, K.J., 1995. Batch test for crushed rocks at pH = 7 distilled waters: a first look at rock impacted aqueous REE signatures. *EOS (Trans. Am. Geophys. Union)* 76, 275, Abstract.